Int. J. Electrochem. Sci., 1(**2006**)324-333

International Journal of ELECTROCHEMICAL SCIENCE
www.electrochemsci.org

Effect of Particle Size on the Electrochemical Capacitance of α-Ni(OH)$_2$ in Alkali Solutions

M. Jayalakshmi[1], *M. Mohan Rao*[1,2]* *and Kwang-Bum Kim*[2]

[1]Inorganic Chemistry Division, Indian Institute of Chemical Technology, Hyderabad-500 007, India
[2]Department of Metallurgical Engineering, Yonsei University, Seodaemoon-gu, Seoul, 120-749, Korea.
*E-mail: mandapati@iict.res.in

Received: 11 August 2006 / *Accepted:* 15 September 2006 / *Published:* 1 October 2006

Effect of nanosized particles of α-Ni(OH)$_2$ in enhancing the electrochemical capacitance as against the microsized particles of the same hydroxide is examined. Nanomaterial was synthesized by hydrothermal method while the micromaterial was prepared by the conventional co-precipitation method. Material characterization was done by XRD, TEM and BET surface area. Electrochemical characterization was carried out by cyclic voltammetry in alkali solutions. The BET surface areas of of nano- and micro-sized α-Ni(OH)$_2$ were shown to be directly proportional to their specific electrochemical capacitance (both faradic and non-faradic) as evident from the values of 20.9 m^2g^{-1}, 289.8 Fg^{-1} and 9.2 m^2g^{-1}, 133.6 Fg^{-1} respectively. Apart from inter-grain conduction, smaller particles increase the shift of conduction and valence band leading to a greater charge separation. An attempt to understand the particle size effect on the enhancement of electrochemical capacitance based on the volume and surface recombination of oppositely charged particles was made.

Keywords: Nanosized α-Ni(OH)$_2$; Pseudocapacitance; Hydrous oxide passive layer; Volume and surface recombination; Supercapacitors

1. INTRODUCTION

Research on nanoparticles synthesis, characterization and applications continues unabated as the nanomaterials make a revolution in macrosystems. Chemically inert gold turns to be catalytically active when the particle size is below 4 nm [1]. The major advantage of nanoparticle assembly over conventional materials is the high surface area to volume ratio. For instance, a nanocrystalline metal oxide may have an internal surface area approximately 1000 times greater than the geometric area which answers for the better capacitances and electronic conductance on exposure to a conducting

electrolyte solution. The existence of such size effects offers a new pathway to regulate reactivity, either chemically or electrochemically or both by controlling the particle size. Electrochemistry plays a key role in nanoparticle science as it paves a way for coupling particle activity to external circuitry.

Fig. 1 shows the effect of particle size on the mechanism of intergrain electron transport for microsized and nanosized particles [2]. In the microsized particles, the depth of space charge layer is insignificant compared to the grain size and the electrical conduction on the application of an external bias is largely governed by the grain boundaries. On the other hand, in nanosized particles, the space charge layer is in par with grain size, so that the application of external bias of same magnitude would have a profound effect on the intergrain conduction, leading to an increase in electronic conduction and thereby, the capacitance. The nanoparticulate surface not only enhances current due to the high surface but also the scale of surface roughness removes the requirement for a solution phase species to mediate electron transfer to the active redox site of the electrode material. Under these conditions, an increase in the electronic and ionic conductance should be inversely proportional to the particle size; i.e. smaller the particle size, higher the conductance and hence the capacitance.

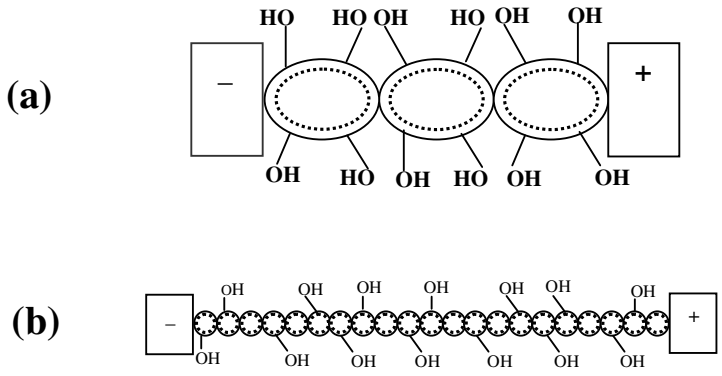

Figure 1. Effect of particle size on the mechanism of intergrain electron transport for (a) microsized, (b) nanosized particles.

A recent work on nano-scale effects in electrochemistry emphasize these points; the catalytic activity of Pd particle increased by two orders of magnitude as the diameter of the single Pd particle on gold electrode decreased from 200 to 6 nm for a electrochemical proton reduction reaction [3]. However, a study on the electrochemical behavior of nanoparticles immobilized on a conducting substrate in the same fashion as conventional particles is more relevant to applications like batteries, super capacitors etc. and the present work aims on it. A recent work on nanometer β-$Ni(OH)_2$ being added to nickel hydroxide electrodes showed that the addition of 8% mass of nanomaterial increased the charge-discharge specific capacity by 10% and this effect was predominant in the initial 100 cycles. The reason attributed was the enhanced proton diffusion in the conversion of Ni^{2+} to Ni^{3+} initiated by the nanomaterial [4]. In the present communication, we have chosen α-$Ni(OH)_2$ as model compound to study the effect of particle size on the electrochemical behaviour. It is a well studied compound that exhibits both faradic charge-transfer and non-faradic capacitances. Its use as battery

and fuel cell electrode is legendary and currently gaining importance as electrode material for pseudocapacitors. Here, we prepared alpha nickel hydroxide particles of (1) nanoscale range by hydrothermal method; (2) conventional microsized particles by co-precipitation method and characterized electrochemically by cyclic voltammetry in 1.0 M NaOH solutions. Material characterization was done by XRD, BET surface area and TEM.

2. EXPERIMENTAL PART

2.1. Nanoparticle synthesis by hydrothermal method:

To synthesize α-$Ni(OH)_2$ nanoparticles, the following procedure was adopted [5]: $Ni(NO)_3 \cdot 6H_2O$ (0.05 M) and urea (0.2 M) were dissolved in 200 ml of de-ionized water and the solution was transferred to a stainless steel autoclave. This was programmed to reach 130 °C in 1 h (ramp time), and at this temperature, the reaction was kept for 2 h (soak time) with a stirring speed of 400 rpm. When the autoclave reached room temperature, the solution with precipitate was filtered, and washed with distilled water to neutral pH. The solid was dried overnight in oven at 120 °C to obtain $Ni(OH)_2$ nanoparticles.

2.2. Micro particle synthesis by co-precipitation

Microsized particles of α-$Ni(OH)_2$ were synthesized as follows: $Ni(NO)_3 \cdot 6H_2O$ (0.03 M) and urea (0.4 M) were dissolved in 100 ml of de-ionized water and the solution was transferred into a round bottomed glass flask, kept for stirring at 90°C on an oil bath for 6 hours. When the reaction mixture reached the room temperature, the precipitate was filtered and washed with distilled water to neutral pH. The solid was dried overnight in oven at 120 ^oC.

For convenience, nanosized and microsized α-$Ni(OH)_2$ samples are designated as n-$Ni(OH)_2$ and b-$Ni(OH)_2$ respectively.

2.3. Instrumentation

All electrochemical experiments were conducted with a PGSTAT 30 Autolab system (Ecochemie, Netherlands). It was connected to a PC running with Eco-Chemie GPES software. GPES software was used for all electrochemical data analysis The reference electrode was an Ag/AgCl (3M KCl) electrode and the counter electrode was a platinum foil supplied along with the instrument. The PIGEs were made by impregnating graphite rods with melted paraffin (mp 65 °C) under vacuum. Paraffin impregnated graphite electrodes (PIGE) were used as working electrodes with the surface immobilized with the active electrode materials. A few micrograms of α-$Ni(OH)_2$ particles were placed on a clean glass plate and the surface of PIGE electrode was pressed over the nanomaterial which would mechanically transfer the nanoparticles to the tip of the electrode [6,7].

Powder XRD data of the samples were obtained by means of a Siemens D 5000 X-ray diffractometer with Bragg-Brentano geometry and having Cu$K\alpha$ radiation (λ=1.5418 Å). Transmission electron microscope (TEM) images were obtained with a PHILIPS make Tecnai-12 FEI

instrument operated at an accelerating voltage of 100 kV. BET surface area was measured by a Quantachrome Autosorb-1 Model.

3. RESULTS AND DISCUSSION

3.1. Material Characterization

XRD spectra of n-$Ni(OH)_2$ and b-$Ni(OH)_2$ show the typical pattern of alpha phase nickel hydroxide whose peaks can be indexed to the standard XRD pattern of α-$3Ni(OH)_2.2H_2O$ (JCPDS 22-0444) and the figures were not given. Fig. 2a and Fig. 2b show the TEM images of b-$Ni(OH)_2$ and n-$Ni(OH)_2$ and the particle sizes range from 150 to 500 nm and 10 to 30 nm respectively. BET surface area of b-$Ni(OH)_2$ was 9.2 m^2g^{-1} and that of n-$Ni(OH)_2$ was 20.9 m^2g^{-1}. These surface areas reflect the geometric values and the actual active surface area would depend on the extent of electrolyte diffusion and wetting of the solid particles by the electrolyte which in turn reflects the electrochemical reactivity of the material. Qualitatively, these values could be considered proportional to the active surface exposed to the electrolyte.

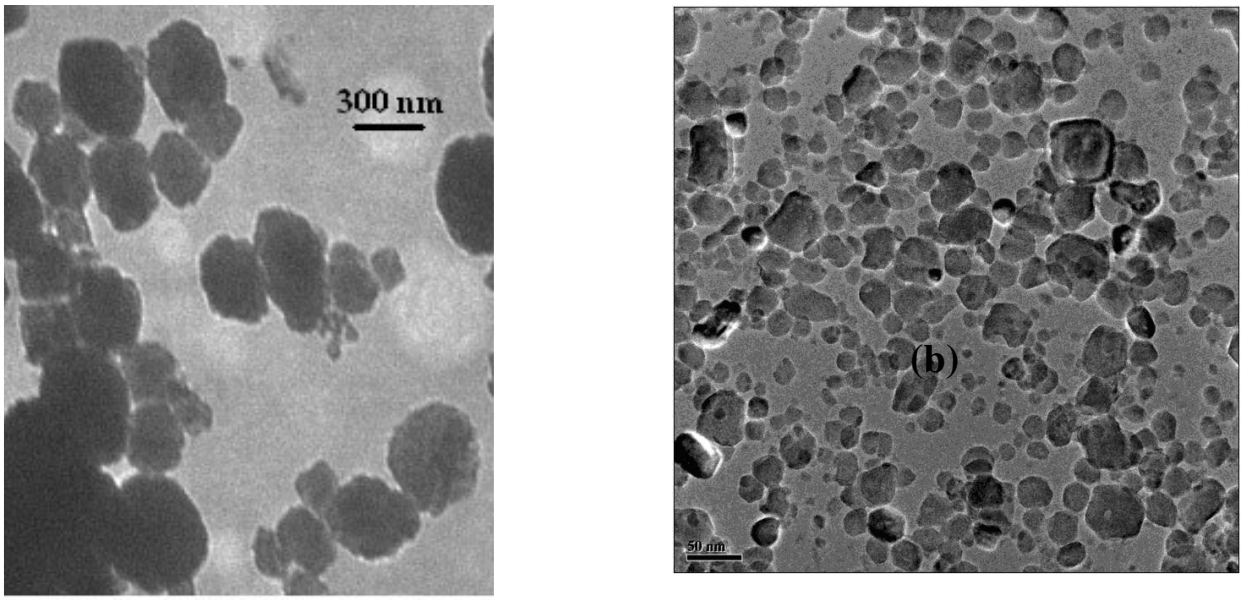

Figure 2. TEM images of α-$Ni(OH)_2$ (a) microsized, (b) nanosized particles.

3.2. Electrochemical Characterization

Figs. 3 and 4 show the cyclic voltammograms (CVs) obtained for alpha phase n-$Ni(OH)_2$ and b-$Ni(OH)_2$ in 1 M NaOH solutions respectively. They were recorded continuously for the consecutive 20 runs. The potential window was extended to -1.5 V in the negative direction in order to study the effect

of particle size on the capacitive behavior of α-$Ni(OH)_2$. The entire potential window from -1.5 to + 0.65 V can be divided into two regions. The plateau region from -1.5 to +0.2 V corresponds to double

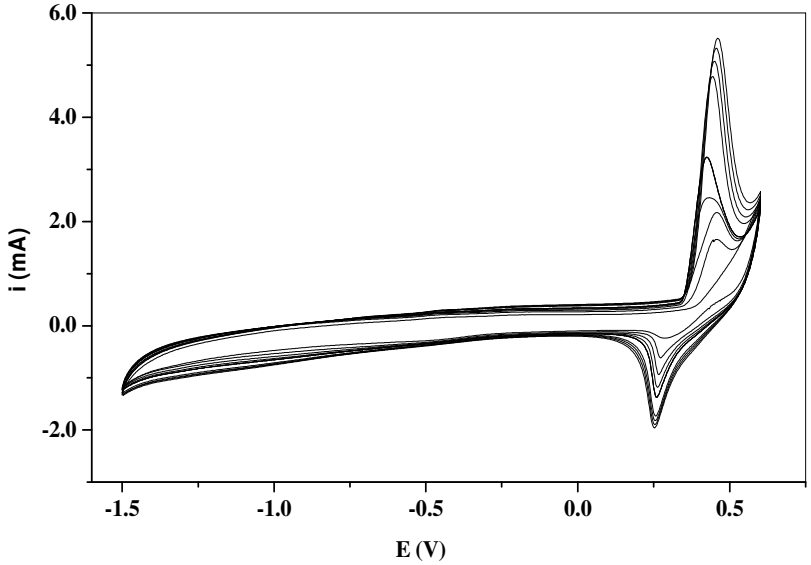

Figure 3. Cyclic voltammograms of bulk $Ni(OH)_2$ in 1.0 M NaOH solutions at the scan rate of 0.05 Vs^{-1}.

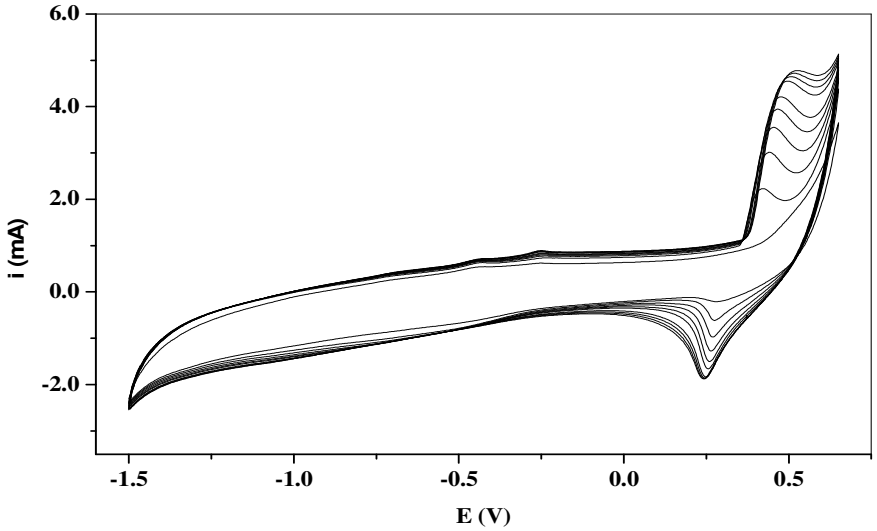

Figure 4. Cyclic voltammograms of nano $Ni(OH)_2$ in 1.0 M NaOH solutions at the scan rate of 0.05 Vs^{-1}.

layer capacitive behavior (Region I) and the peak region from +0.2 to 0.6 V corresponds to the faradic charge transfer reaction (Region II). The redox peaks are due to the proton insertion and de-insertion reaction well documented in the course of studies for Ni electrode rechargeable batteries.

$$Ni(OH)_2 \leftrightarrow NiOOH + H^+ + e^-$$

Though the redox transformation remains the same for both n-$Ni(OH)_2$ and b-$Ni(OH)_2$ samples, the difference in peak shapes and anodic peak potentials indicate a definite distinction in the redox

behaviour that could be attributed to solely particle size. For better visualization, a typical cyclic voltammogram (5^{th} scan) for both samples was singled out and presented in Fig. 5 and the parameters obtained from the same curves were presented in Table 1. At first sight, it was clear that the peak shapes especially that of anodic were different; for b-$Ni(OH)_2$, the peaks were sharper indicating a dominance of charge transfer control while for n-$Ni(OH)_2$, the peaks have a diffusion tail suggesting a mass transfer dominance in the redox mechanism.

Table 1. Parameters derived from the CVs of nanosized and microsized α-$Ni(OH)_2$ for the 5^{th} scan at the scan rate of 0.05 Vs^{-1}

Parameter	n-$Ni(OH)_2$	b-$Ni(OH)_2$
Anodic peak potential	0.451 V	0.421 V
Cathodic peak potential	0.260 V	0.260 V
Anodic peak charge	3.855×10^{-3} C	4.161×10^{-3} C
Cathodic peak charge	1.285×10^{-3} C	3.344×10^{-3} C
Q_a/Q_c	1.227	1.244
Anodic charge (Region I)	1.060×10^{-2} C	3.727×10^{-3} C
Polarization resistance (R_p) at (a) HER (-1.0 V) (b) OER (+0.43 V)	6.551×10^{2} ohm 1.406×10^{2} ohm	1.479×10^{3} ohm 2.087×10^{2} ohm
Specific capacitance	294.9 Fg^{-1}	133.6 Fg^{-1}

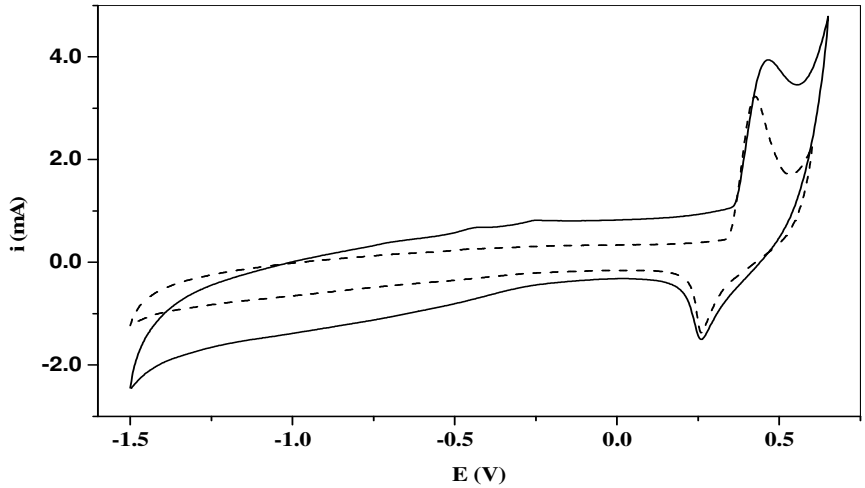

Figure 5. Cyclic voltammograms of α-$Ni(OH)_2$ at the 5^{th} scan: - - bulk $Ni(OH)_2$; —— nano $Ni(OH)_2$ in 1.0 M NaOH at the scan rate of 0.05 Vs^{-1}.

Though the cathodic peaks occur at the same potentials in both the samples, the anodic peak appeared 30 mV more positive in n-$Ni(OH)_2$ as compared to b-$Ni(OH)_2$ indicating the oxidation of Ni^{2+} to Ni^{3+} occurs more readily if the particle sizes were in the nanoscale range. Electrochemical ageing of alpha to beta phase of $Ni(OH)_2$ being a common feature in both the samples, the shift in peak potentials can be safely asserted to the particle size. It was interesting the cathodic peak potential remain unaffected by the particle size factor, though the peak shapes appear to be more broadening in the case of n-$Ni(OH)_2$ as against that of b-$Ni(OH)_2$. Q_a/Q_c ratio (1.2) remains almost the same for both samples indicating the oxidation step involves more than one electron as expected for α-$Ni(OH)_2$ but the charge under the oxidation peak for n-$Ni(OH)_2$ was an order increase than that of b-$Ni(OH)_2$, thus confirming the significance of smaller particles. Also the Rp (polarisation resistance) seem to be lower for the hydrogen evolution process of n-$Ni(OH)_2$ than that of b-$Ni(OH)_2$ which is consistent with the earlier report [4].

An order increase in anodic charges for nanosized alpha nickel hydroxide as shown in Table 1 confirms the importance of nanosized particles in increasing the electrochemical capacitance of α-$Ni(OH)_2$. This happens as a result of increase in ion concentration at the electrode/surface interface which is directly proportional to the polarization of $Ni(OH)_2$ electrodes and surface area of the electrochemically active particles. As water plays a crucial role in the electrochemistry of nickel hydroxide, the increase in surface area of nanoparticles increases the adsorption ability of water molecules to adhere to the surface via hydrogen bonds. This surface water improves the wettability of nickel hydroxide nanoparticles, thus resulting in an enhanced proton transport within the active material during the redox transformation. In Region II, not only double layer capacitance but also pseudocapacitance arises. The electrochemical behaviour of α-$Ni(OH)_2$ in this region is similar to the capacitative behaviour of hydrous RuO_2 where it arises on account of several overlapping redox processes involving proton and electron injection (or removal) that remain highly reversible because no phase change occurs. The mirror-image profile of CVs in Figs. 3 and 4 confirm the reversible characteristics of pseudocapacitance oxidation-reduction profile.

In an aqueous alkali solution, it was known that nickel is covered with an oxide-hydroxide layer which is hydrated to a varying degree and whose stoichiometry, oxidation degree and proton content depend on electrode potential and electrode history. It was shown if the nickel electrode was first polarised at -1.2 V Hg-HgO, the passive layer formed on the surface of nickel electrode consisted of α-$Ni(OH)_2$ which gets oxidized at -0.6 V and reduced at -0.9 V provided the potential was limited up to -0.35 V. When the upper limit of the sweep was increased to 0.6 V, the peak potential was progressively shifted towards negative potentials: for an upper limit of 0.6V Hg-HgO, this reduction peak did not appear as the conversion of alpha to beta phase takes place in this potential domain [8]. On anodic polarisation starting from -1.5 V as in the present study, the following oxidation reaction may possibly occur in the hydrous oxide layer [9].

$$3Ni(OH)_2 .xH_2O \leftrightarrow Ni_3O_2(OH)_4.xH_2O + 2H^+ + 2e^-$$

$$Ni_3O_2(OH)_4.xH_2O + OH^- \leftrightarrow 3NiOOH + (x+1)H_2O + e^-$$

Both reactions are chemically and electrochemically reversible. At this junction, the reasoning that the promotion of proton diffusion in increasing the electrochemical performance of nanosized particles claimed in the earlier work by X. J. Han et al could be valid for the observations in this work [4].

The specific capacitance for the entire process on the anodic scan was 289.8 Fg^{-1} for n-$Ni(OH)_2$ and 133.6 Fg^{-1} for b-$Ni(OH)_2$ at the scan rate of 50 mVs^{-1}. The specific capacitance was calculated according to the equation [10]:

$$C = Q/m\upsilon\Delta V$$

where Q (Coulombs) is the total charge combining both faradic and double layer components, m is the mass in grams, υ the scan rate (Vs^{-1}) and ΔV is the potential window in volts. The voltage window was taken between the limits of hydrogen and oxygen evolution onset potentials.

It is clear from the CVs in Fig. 5 that there is noticeable increase in charges flowing under the curves for n-$Ni(OH)_2$ as against b-$Ni(OH)_2$ and the reason for this enhancement could be attributed to solely the particle sizes of alpha phase nickel hydroxide. The tailing anodic peak of n-$Ni(OH)_2$ indicates the accessibility of electrolyte by diffusion amongst the nanoparticle which is a prerequisite for materials that show characteristics of supercapacitors rather than batteries. Effect of nanoparticles on the enhancement of electrochemical activity has been reported by several authors but the mechanism of the size effect on the reactivity is not probed. In photo catalytic studies, theoretical models and experimental investigations have led to the discovery that an optimum particle size of TiO_2 is a much needed requisite to enhance the photo catalytic rates to a maximum. Gerischer developed a model based on which the quantum yield (defined as the ratio of electron-hole pairs involved in the redox reaction at the surface of particle to total electron-hole generated) increases as the particle size decreases from 1000 to 10 nm [11]. In this model, surface recombination is presumed to occur at a faster rate owing to the smaller particle. In semiconductors, band gaps were found to be particle size dependent and $Ni(OH)_2$ is well known as a p-type semiconductor [12]. Chemical reactivity increased as the particle size decreased. For ZnO nanoparticles, the maximum reactivity with the catechols has been observed for the smallest size particles [13]. However, this is not universally true. There are exceptional reactions where the larger clusters were more efficient in promoting the reactions such as photoinitiated polymerization of methyl methacrylate [14]. Grela and Colussi developed a model which predicted that quantum yield increased with particle size because the electron-hole recombination rates at the surface were slower [15].

Based on these observations, the particle size effect on the enhanced charges under the CV curves of nano-nickel hydroxide could be reasoned as due to the faster electron-hole recombinations at the surface of the particle as depicted in Fig. 6 [11]. There are two processes that take place on the application of external bias to the α-$Ni(OH)_2$ particles. The electrical field that exceeds the band gap of the $Ni(OH)_2$, results in primary charge separation. The smaller the size of the particle, greater is the shift of conduction and valence band towards more negative and positive potentials respectively i.e. greater charge separation. The positive and negative charges may recombine in two ways (1) volume recombination within the particle (2) surface recombination at the surface of the particle. In smaller

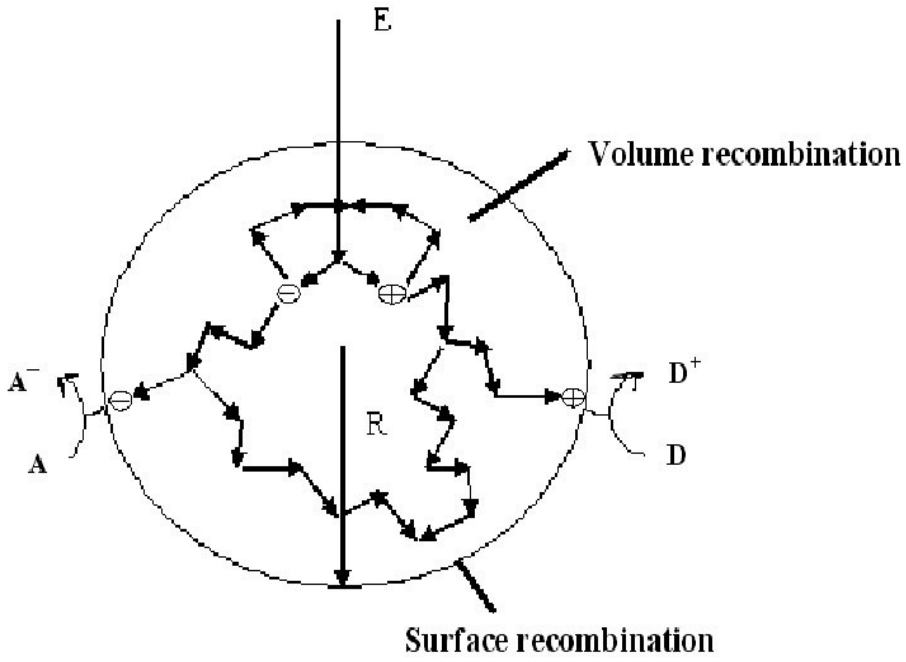

Figure 6. Pictorial representation of particle size effect determined by volume recombination and surface recombination of holes and electrons.

particles, process 2 dominates while in larger particles, process 1 dominates. Most electrons and holes generated inside the particle can reach the surface only if the size of the crystal is less than 300 nm. For a semiconductor-electrolyte interface, the interfacial capacitance can be subdivided into serial capacitances including the space-charge capacitance on the semiconductor side and the double layer capacitance on the electrolyte side. In a strong electrolyte, such as in the present case (1M KOH *(*aq*)*), the capacitance of the entire system closely approximates to the space–charge value on the semiconductor side. In this case, the Mott-Schottky relationship predicts an interfacial capacitance (per unit surface area) increase with the carrier density of the semiconductor. The same effect extends to the grain conductivity, and hence to the responding behavior of the electrode to the charging-discharging protocol.

4. CONCLUSIONS

In summary, nanoparticles enhance the pseudocapacitance of α-$Ni(OH)_2$ to a two-fold increase as compared to microsized particles of the same hydroxide. For the stabilized CV, we achieved a maximum specific capacitance of 289.8 Fg^{-1} for nanosized and 133.6 Fg^{-1} for microsized α-$Ni(OH)_2$ emphasizing the importance in size reduction of particles. Though the particles tend to agglomerate with continuous cycling as observed in earlier reports, the higher capacities that could be drawn in the initial cycles of charge-discharge is worth the effort and makes the use of nanosized particles in electrodes, an attractive and benefical exercise.

ACKNOWLEDGMENT

This work was financially supported by the Ministry of Education and Human Resources Development (MOE), the Ministry of Commerce, Industry and Energy (MOCIE) and the Ministry of Labor (MOLAB) through the fostering project of the Lab of Excellency and by the ERC program of MOST/KOSEF (Grant No. R11-2002-102-00000-0). M. M. Rao thanks KOFST, Republic of KOREA for Brain Pool Fellowship.

References

1. M. Valden, X. Lai, D. W. Goddman, *Science,* 281(1998)1647
2. G. Williams, G. S. V. Coles, *J. Mater. Chem.,* 8(1997)1657
3. J. Meier, J. Schiøtz, P. Liu, J. K. Nørskov, U. Stimming, *Chem. Phys. Lett.,* 390(2004)440
4. X. J. Han, P. Xu, C. Q. Xu, L. Zhao, Z. B. Mo, T. Liu, *Electrochim. Acta,* 50(2005)2763
5. M. Jayalakshmi, N. Venugopal, B. Ramachandra Reddy, M. Mohan Rao, *J. Power Sources,* 150(2005)272
6. F. Scholz, B. Meyer, Voltammetry of solid microparticles immobilized on electrode surfaces. In A. J. Bard and I. Rubinstein (eds.) Electroanalytical chemistry, a series of advances, Vol. 20, Dekker, New York, 1998
7. M. Jayalakshmi, M. Mohan Rao, F. Scholz, *Langmuir*, 19(2003)8403
8. G. Barral, F. Njanjo-Eyoke, S. Maximovitch, *Electrochim. Acta*, 40(1995)2815
9. V. S. Muralidharan, N. Jayalakshmi, P. Mageswari, *Bull. Electrochem.,* 7(1991)355
10. B. E. Conway, Electrochemical Supercapacitor, Kluwer Academic/Plenum publishers, New York, 1999.
11. H. Gerischer, *Electrochim. Acta,* 40(1995)1277
12. G. Barral**,** F. N. Eyoke, S. Maximovitch, *Electrochim. Acta*, 40(1995)2815
13. G. Ramakrishna, H. N. Ghosh, *Langmuir,* 19(2003)3006
14. G. Mills, M. R. Hoffmann, *Environ. Sci. Technol.,* 27(1993)1681
15. M. A. Grela, A. J. Colussi, *J. Phys. Chem.*, 100(1996)18214

© 2006 by ESG (www.electrochemsci.org)